Available online at BCREC website: https://bcrec.id

Bulletin of Chemical Reaction Engineering & Catalysis, 17 (3) 2022, 565-576

Research Article

Comparative Adsorption Performance of Carbon-containing Hydroxyapatite Derived *Tenggiri* (*Scomberomorini*) and *Belida* (*Chitala*) Fish Bone for Methylene Blue

Sri Lestari[1], Mukhamad Nurhadi[1,*], Ratna Kusumawardani[1], Eko Saputro[1], Retno Pujisupiati[1], Nova Sukmawati Muskita[1], Nezalsa Fortuna[1], A'an Suri Purwandari[1], Fahria Aryani[1], Sin Yuan Lai[2,3,4], Hadi Nur[5,6]

[1]*Department of Chemical Education, Universitas Mulawarman, Kampus Gunung Kelua, Samarinda, 75119, East Kalimantan, Indonesia.*

[2]*School of Energy and Chemical Engineering, Xiamen University Malaysia, Selangor Darul Ehsan 43900, Malaysia.*

[3]*College of Chemistry and Chemical Engineering, Xiamen University, Xiamen 361005, China.*

[4]*Kelip-kelip! Center of Excellence for Light Enabling Technologies, School of Energy and Chemical Engineering, Jalan Sunsuria, Bandar Sunsuria, 43900 Sepang, Selangor Darul Ehsan, Malaysia.*

[5]*Department of Chemistry, Universitas Negeri Malang, Malang 65145, Indonesia.*

[6]*Center of Advanced Materials for Renewable Energy (CAMRY), Universitas Negeri Malang, Jl. Semarang No. 5, Malang 65145, Indonesia.*

Received: 24th July 2022; Revised: 31st August 2022; Accepted: 1st September 2022
Available online: 10th September 2022; Published regularly: September 2022

Abstract

The utilization of fishbone as the carbon source for methylene blue adsorption has been successfully studied. Fishbone was prepared from two kinds of fish such as marine fisheries (ex. *Tenggiri*) and freshwater fisheries (ex. *Belida*). The carbons were prepared by carbonation of fishbone powder at 500 °C for 2 h. Physical properties of carbons were characterized using Fourier transform infrared (FTIR) spectroscopy, X-ray diffraction (XRD), wavelength dispersive X-ray fluorescence (WDXRF), Scanning Electron Microscope (SEM), and hydrophobicity. The carbons were utilized as the adsorbent for removing methylene blue by varying the contact time, initial dye concentration, and temperature. It is concluded that both carbons can very good adsorb the methylene blue. The adsorption performance of carbon (TFC) from *Tenggiri* fish is better than carbon (BFC) from *Belida* fish. The adsorption was well fitted with the Langmuir adsorption model (R^2 ~ 0.998) and the pseudo-second-order model. This indicated that the dye molecules were adsorbed on the surface-active site of carbon via chemical binding, forming an adsorbate monolayer. Thermodynamic parameters, including the Gibbs free energy (ΔG), enthalpy (ΔH), and entropy (ΔS), indicated that the adsorption of methylene blue onto the carbon from fishbone was spontaneous. Thus, carbon from fishbone can be applied as a low-cost adsorbent to treat industrial effluents contaminated with methylene blue.

Keywords: Fishbone; Carbon; Methylene blue; Carbonization; Adsorption

How to Cite: S. Lestari, M. Nurhadi, R. Kusumawardani, E. Saputro, R. Pujisupiati, N.S. Muskita, N. Fortuna, A.S. Purwandari, F. Aryani, S.Y. Lai, H. Nur (2022). Comparative Adsorption Performance of Carbon-containing Hydroxyapatite Derived Tenggiri (*Scomberomorini*) and Belida (*Chitala*) Fish Bone for Methylene Blue. *Bulletin of Chemical Reaction Engineering & Catalysis*, 17(3), 565-576 (doi: 10.9767/bcrec.17.3.15303.565-576)

Permalink/DOI: https://doi.org/10.9767/bcrec.17.3.15303.565-576

1. Introduction

The development of industries that require synthetic dyes, such as the textile, paper, rubber, plastics, leather, cosmetic, pharmaceutical and food industries, is very fast in the world. Consequently, a lot of waste pollution is produced, which can damage the environment. The synthetic dye compounds are very stable, so it difficult to decompose, and they can be carcinogenic and has high toxicity to the environment

* Corresponding Author.
Email: nurhadi1969@yahoo.co.id (M. Nurhadi);
Telp.: +62 81346482251; Fax: +62 541 743929

[1–3]. Research efforts in degrading methylene blue as synthetic dyes are often carried out using many adsorbents. Adsorption is a familiar separation technique known since the earlier history of science and is considered as an efficient and user-friendly method for eliminating a wide range of toxic pollutants from wastewater. Adsorption is a physicochemical method of treating aqueous effluent that is rapidly gaining prominence due to its proven efficiency and great potential as means of producing quality effluent [4–6]. Many purposes of separation and purification with the adsorption technology have been used extensively in industrial processes. An essential application of adsorption process using suitable adsorbents is considered in the removal of coloured and colourless organic pollutants from industrial wastewater [7].

Recently, many researchers have been efforted to find cheaper and more efficient alternative materials as dyes adsorbent, such as agricultural residues [8], clay minerals [1,3], cashew nut shell [2], fly ash [9], peat [10], yellow passion fruit peel [11], wood powder and lignin [12,13]. However, the cost of its commercial application is still very high and low efficiency. Indonesian country is the largest tropical archipelagic country in the world which has a vast ocean and a large number of many large and small islands. The potential of the Indonesian fishery sector is the largest in the world, including capture fisheries (ex. *Tenggiri (Scomberomorini*)) and aquaculture (ex. *Belida (Chitala*)) with a sustainable production potential of around 67 million tons/year [14,15]. The consequence of abundant fish yields is that large amounts of fish bone waste have been produced. The compositions of fish bone waste are composed of calcium phosphate, collagen fiber, calcium carbonate, and hydroxyapatite [16,17], which are very useful for several applications, namely photocatalysts [18,19], catalysts [20,21], adsorbents [22–24], *etc*. Captivated by the high carbon-containing hydroxyapatite of the fish bone, our research team has explored the usage of modified fish bone as a catalyst in styrene oxidation [15,25] and an adsorbent in methylene blue removal [26,27].

In this study, we have modified fish bone to be the highly adsorptive carbon source as an adsorbent to remove methylene blue dye from the wastewater. Firstly, the fish bone was ground to powder and then activated by thermal activation at 500 °C for 2 h. The carbon was characterized by FTIR, XRD, XRF, SEM, Nitrogen adsorption-desorption, and hydrophobicity. Finally, the carbon will be tested to adsorb methylene blue on the effect contact time variation for the kinetic study and the initial methylene blue concentration effect for Langmuir and Freundlich isotherm studies. Furthermore, variation temperature for investigating thermodynamic parameters was also carried out.

2. Materials and Methods

2.1 Carbonation Process

Tenggiri (Scomberomorini) and *Belida (Chitala)* fish bone were obtained from food company in Samarinda, East Kalimantan, Indonesia. The fish bones were washed with boiling water to separate them from other impurities. The fish bone was dried in an oven at 110 °C for overnight and it was crushed to fine powder. The powder was carbonized in a furnace at 500 °C for 2 h in an air atmosphere to form carbon. The fish bone-derived carbon is labelled as TFC for *Tenggiri* fish bone and BFC for *Belida* fish bone.

2.2 Carbon Characterization

The samples were characterized by using WDXRF, FTIR, XRD, SEM-EDX, BET adsorption-desorption and Hydrophobicity. The elements composition from the carbon was determined by using 1 kW wavelength dispersive X-ray fluorescence (WDXRF PANalytical, Minipal 4). FTIR spectrometer (IR−Prestige−21 Shimadzu) was used to identity the functional group in the sample with a spectral resolution of 2 cm^{-1}, scans 10 s, at 20 °C and range of wavenumber from 400 to 4000 cm^{-1}. XRD instrument (Phillips PANalytical X'Pert PRO) was used to determine of the crystallinity and phase content of the sample with the Cu K_α (λ = 1.5406 Å) radiation as the diffracted monochromatic beam at 40 kV and 40 mA and the pattern was scanned in the 2θ ranges between 7° and 60° at a step 0.03° and step time 1 s. SEM (FEI Inspect S50) instrument was used to investigate the surface morphology of sample with an accelerating voltage of 15 kV. The hydrophobicity was correlated with the amount adsorbed water in the samples. In an experiment, samples (1 g) were dried at 110 °C overnight in an oven to remove all physically adsorbed water. Distillated water (0.75 L) was filled into desiccators for overnight. After dehydration, the samples were exposed to water vapor by placing them into the water-filled desiccators at room temperature and weighed every 30 min. The percentage of adsorbed water as a function of time was determined follow the Equation (1):

$$\%adsorbed\ water = \frac{(m_t - m_0)}{m_0} \times 100 \quad (1)$$

where, m_t represents the sample mass after adsorption of water and m_0 represents the initial mass of the sample.

2.3 Adsorption Test

The performance of adsorbent was tested using methylene blue ($C_{16}H_{18}ClN_3S.xH_2O$, x = 2–3, Merck) dyes. The methylene blue structure was shown in Figure 1. The adsorption was carried out by mixing 0.250 g of the adsorbent with 25 mL of methylene blue solution (100 mg.L^{-1}) in a 100 mL beaker glass at room temperature for the duration of 5, 10, 15, 20, 25, 30, 60, 120, and 240 min. Furthermore, the adsorbent was separated from the filtrate by centrifugation, and the residual dye in the filtrate was analyzed using UV-vis spectrophotometer by monitoring the changes in absorbance at 660 nm for methylene blue. The effect of initial dye concentration was investigated by varying initial concentrations 100, 200, 300 and 400 mg.L^{-1}. In this study, the thermodynamic parameters (enthalpy, entropy and free energy) were also investigated following the adsorption data of the effect of temperature (30, 40 and 50 °C).

The adsorption efficiency of the adsorbent was determined following this equation (2) [28,29]:

$$Adsorption\ efficiency\ (\%) = \frac{(C_0 - C_t)}{C_0} \times 100 \quad (2)$$

where, C_0 is the dye initial concentration and C_t is the dye concentration after adsorption time t (mg.L^{-1}) in the solution. The adsorption capacity q_t of adsorbent (mg/g) was calculated with following the Equation (3) [5,30]:

$$q_t = \frac{(C_0 - C_t)V}{W} \quad (3)$$

where, V is the volume of dye solution (mL) and W is weight adsorbent (g).

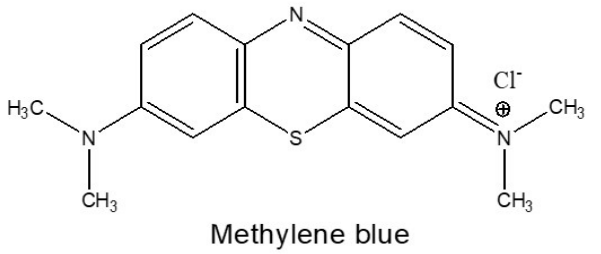

Methylene blue

Figure 1. The chemical structure of dye.

3. Results and Discussion

3.1 Physical Properties

The results from wavelength dispersive X-ray fluorescence (WDXRF) show that both of samples were consisted of major elements calcium (Ca) and phosphorus (P). Both of the samples also consist the transition metal as minor constituents which are ferrum (Fe), cuprum (Cu), and zinkum (Zn). The complete list of elements and compounds was displayed in Table 1.

The FTIR spectra of (a) HA, (b) BFC and (c) TFC are shown in Figure 2. The wavenumber to detect the functional group of hydroxyapatite (HA) were measured in range 4000 to 400 cm^{-1}. All of the spectra show the absorption bands around 2500–3600 cm^{-1} corresponded to the stretching mode of hydroxyl (O−H) group of organic compounds. The HA in the sample was proven by the presence of carbonate ion (CO_3^{2-}) and phosphate ion (PO_4^{3-}) groups [16,31–35]. The C−O stretching was investigated by the absorption bands at 1449, 1272 and 877 cm^{-1} which correlated with the carbonate ion (CO_3^{2-}). The phosphate group (PO_4^{3-}) absorption band were characterized from wavenumber 1150 to 460 cm^{-1}. The P−O stretching asymmetric was identified by the absorption bands around 1150–1000 cm^{-1} which correlated with the phosphate ion (PO_4^{3-}). The bending vibration of PO_4^{3-} was observed by bands located at 620–510 cm^{-1}. The bands at 877 cm^{-1}, which was assigned to the acidic phosphate group (HPO_4^{2-}) [36].

The crystallinity of (a) HA, (b) BFC and (c) TFC were shown by using the XRD pattern in Figure 3. In Figure 3(a), the crystallinity

Table 1. Elements analysis of BFC and TFC obtained using WDXRF.

Element (wt%)	BFC	TFC
P	16.3	17.3
Ca	81.2	79.5
Fe	0.08	0.09
Cu	0.04	0.04
Zn	0.03	0.10

(JCPDS-PDF 74-0565) of HA powder was shown by the diffraction peaks at 2θ = 25.8°, 28.8°, 31.6°, 32,8°, 33.9°, 39.7°, 46.6°, 47.8°, 49.4°, 50.4°, 51.3°, 52.1°, and 53.1° which correspond to (002), (210), (211), (300), (212), (310), (311), (312), (213), (004), (104), and (322) sets of planes respectively manifested that the obtained samples were of pure form of hydroxyapatite with hexagonal structure [16,17]. In Figure 3(b) and 3(c), the crystallinity (JCPDS-PDF 74-0565) can be investigated by the diffraction peaks at 2θ = 25.7°, 28.8°, 32.8°, 39.7°, 46.6°, and 49.4°. The diffraction peaks in Figure 3(b) and 3(c) are not clear due to HA crystal still mixed with carbon. The XRD in Figure 3(b) and 3(c) did not show any other peaks corresponding to secondary phases or intermediate compounds, such as $CaHPO_4.2H_2O$ or $Ca_8(HPO_4)_2(PO_4)_4.5H_2O$. The percentage of crystallinity and amorphous of BFC and TFC was calculated by using OriginPro 2021 the Ultimate Software for Graphing & Analysis. The percentage of amorphous of BFC was higher than TFC. The percentage of crystallinity and amorphous was displayed in Table 2.

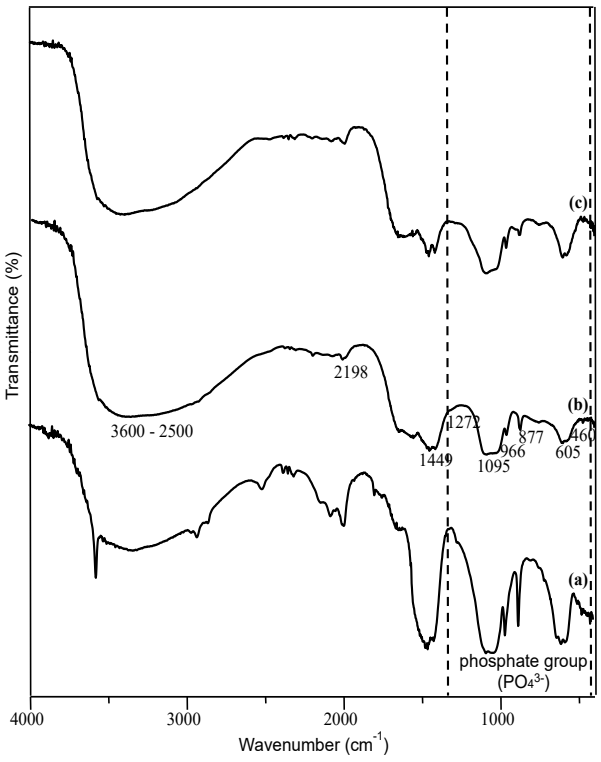

Figure 2. FTIR spectra of (a) HA (b) BFC and (c) TFC.

Figure 4 shows the SEM images of BFC and TFC. In Figure 4, the surface morphology of both of samples are roughness and irregular. The particle size of TFC appears bigger than BFC.

The analysis of Nitrogen adsorption-desorption isotherm was used to determine the surface area and pore structure of all samples. Figure 5 shows nitrogen adsorption-desorption isotherms of TFC and BFC. Both isotherms were of Type IV in the IUPAC classifications, which are a typical isotherm for mesoporous materials. The isotherms exhibited that hysteresis loops in the relative pressure range ~0.4–1.0 for TFC and BFC. The surface area, pore volume and mean pore size completely can be seen in Table 2. Mean pore size of both samples more than 2 nm indicates the presence of uniform mesopores. Surface area of BFC higher than TFC, it was caused the particle size of TFC bigger than BFC that can be proven in SEM images. Figure 6 shows percentage of adsorbed water of BFC and TFC. The percentage of adsorbed water of TFC was significantly higher than BFC. It indicates that BFC more hydrophobic than TFC. From the SEM results,

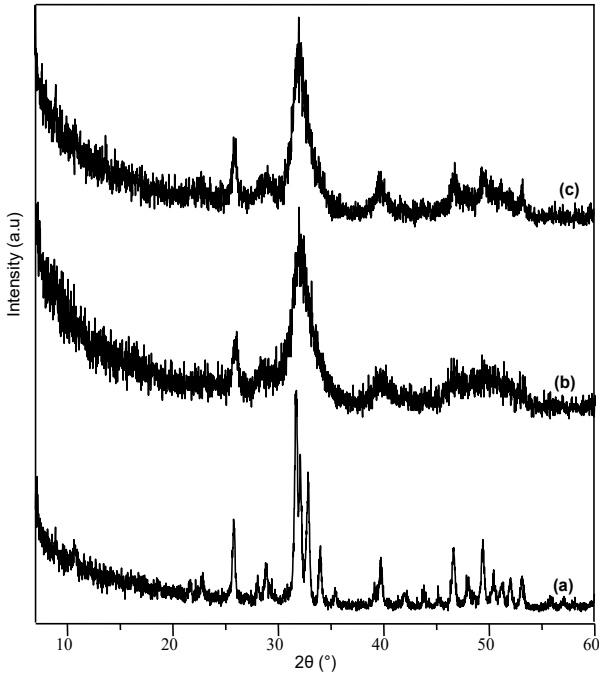

Figure 3. XRD pattern of (a) HA, (b) BFC and (c) TFC.

Table 2. Physical properties of BFC and TFC.

Samples	BET surface area (m^2/g)	Pore Volume (cm^3/g)	Mean pore size (nm)	Crystalinity (%)	Amorphous (%)
BFC	131.7	0.2581	4.3	25.6	74.4
TFC	90.8	0.2369	5.2	26.9	73.1

it can be shown that the particle size of BFC is smaller than TFC so that BFC is very difficult to contact with water as a solvent for methylene blue. From the XRD results, we can determine the percentage of amorphous carbon of BFC is ~75% higher than TFC (~73%), the higher percentage of amorphous carbon causes BFC is difficult to contact with water as methylene blue solvent.

Table 3 shows that the methylene blue adsorption capacity is affected by three factors, *i.e.* surface area, active sites, and targeted sorbents. The torrefied rice husk, which is low in surface area and scarce of active sites, gave low adsorption capacity [6]. Although TiO_2-sulfonated carbon-derived from *Eichhornia crassipes* is comparatively high in surface area and functionalized with functional groups, it gave low adsorption capacity due to this adsorbent is selective to anionic dye (Congo Red) but not cationic dye (Methylene Blue) [26]. Astonishingly, graphene oxide/alginate displayed relatively low surface area but contributed a high removal ability [41], this owing to its abundance of active functional groups. Bamboo-based activated carbon, which consists of plentiful active sites and high surface area, showed very good methylene blue removal capability [43]. Our current study with pristine carbon-derived fish bones gave good adsorption capacities because of the charge interaction, whereby the hydroxyapatite functional groups, *i.e.* CO_3^{2-} and PO_4^{3-} groups, could be attracted to S^+ and N^+ from cationic methylene blue. Nonetheless, the carbon-derived fish bones can be further improved by Van der Waals force by functionalizing with aromatic-structured, polymeric compounds to remove the heterocyclic aromatic methylene blue effectively.

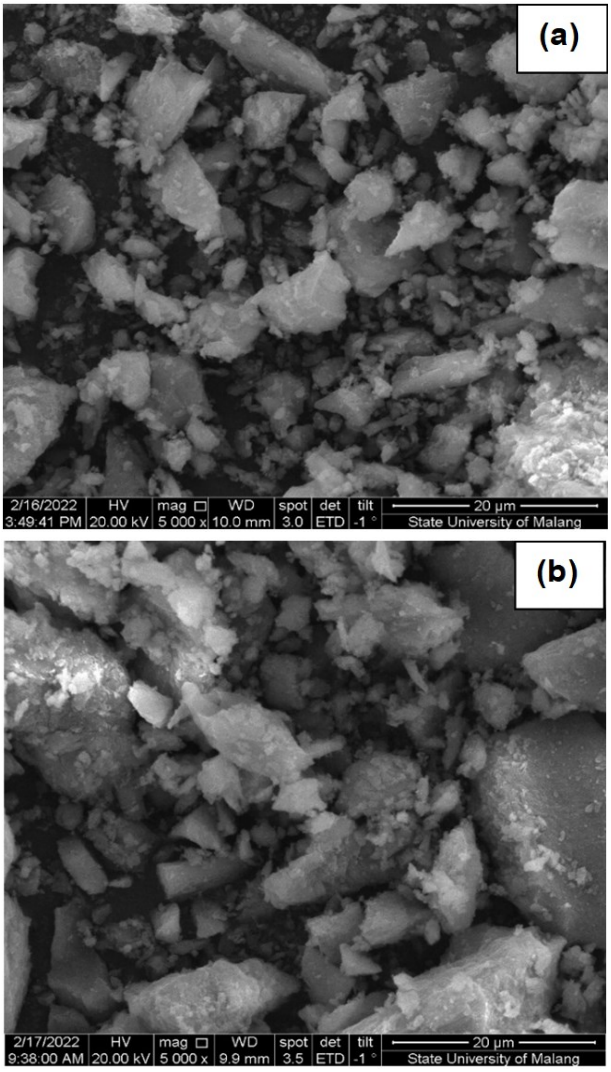

Figure 4. SEM Image of (a) BFC and (b) TFC.

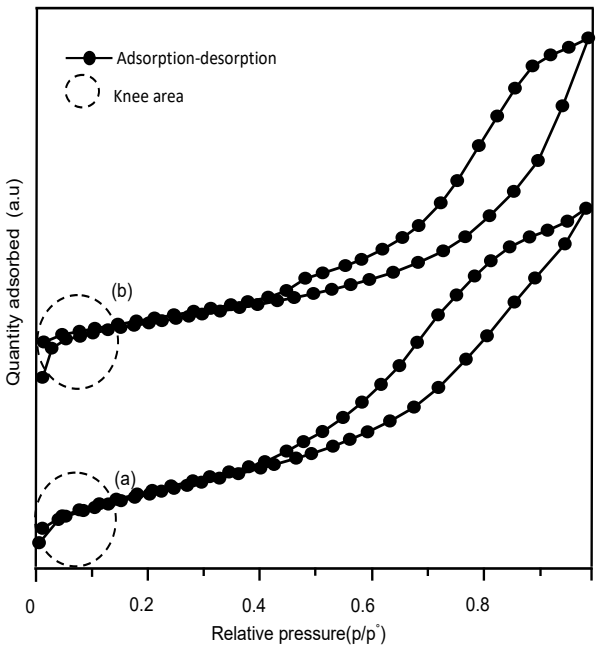

Figure 5. The physisorption isotherms of (a) BFC and (b) TFC.

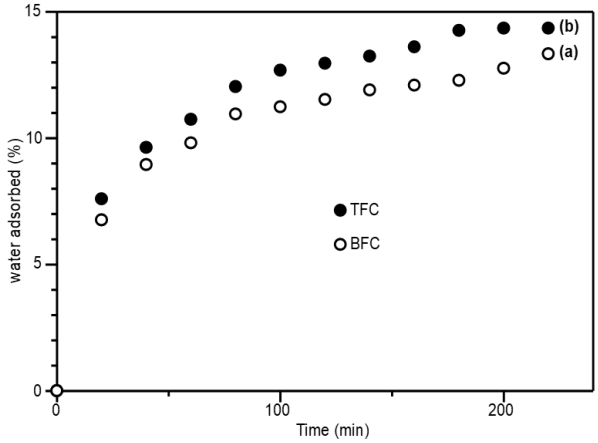

Figure 6. Hydrophobicity of (a) BFC and (b) TFC.

3.2 Effect of Contact Time

The effect of contact time on the percentage dye removal of methylene blue onto TFC and BFC adsorbents are shown in Figure 7. These results indicate that the equilibrium adsorption such as ~90% for BFC and ~98% for TFC was reached within 20 min by both adsorbents and dye removal percentage increased with increasing contact time. Both adsorbents rapidly adsorbed methylene blue within the first 5 min of contact time with adsorption capacity of ~85% for BFC and ~94% for TFC. The changes in adsorption capacity increased gradually until the equilibrium was achieved within 20 min. The dye removal by BFC is lower than of TFC, most probably caused by the physical properties such as the hydrophobicity, which was BFC more hydrophobic than TFC. The solvent for methylene blue is distillate water, this makes it difficult for hydrophobic carbon to make contact with the solution and may have hindered the effective adsorption of the methylene blue onto the surface of the adsorbent. Furthermore, after adsorption duration time 240 min the equilibrium methylene blue achieved 92.8% for BFC and 99.7% for TFC.

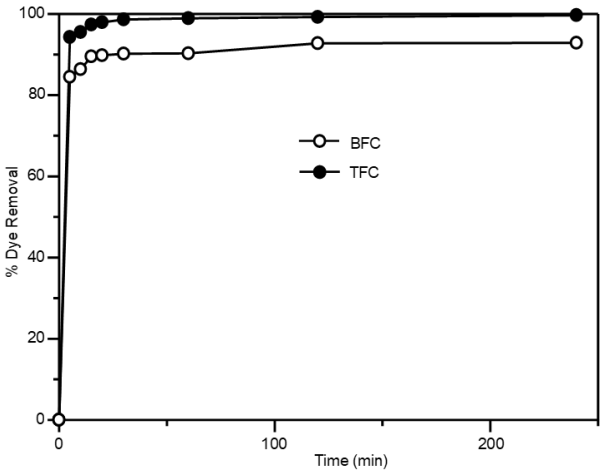

Figure 7. Effect of contact time on the % of methylene blue dye removal on TFC and BFC Conditions: (neutral pH of dye solution: 100 mg.L^{-1}, weight adsorbent: 250 mg, at 30 °C).

3.3 Adsorption Kinetics

The pseudo-first-order kinetic models and the pseudo-second-order kinetic model were use to check the adsorption kinetic of methylene blue adsorption onto TFC and BFC adsorbent. The pseudo-first-order kinetic models by Lagergren base on the sorption capacity of adsorbent is expressed as [45–47]:

$$\ln\left(q_e - q_t\right) = \ln q_e - k_1 t \tag{4}$$

where, k_1 (g/mg.h) is the rate constant for Lagergren pseudo first-order, q_e and q_t are the amounts of dye adsorbed per gram of adsorbent (mg/g) at equilibrium and any time t. The slope and intercept from plot $\ln(q_e - q_t)$ versus t was used to determine the value of k_1 and q_e.

The pseudo-second-order kinetic model by Ho, Y. S., and McKay, G is also based on the sorption capacity of the adsorbent with the equation [48–49]:

$$\frac{t}{q_t} = \frac{1}{k_2 q_e^2} + \frac{t}{q_e} \tag{5}$$

where, k_2 (g.mg^{-1}.h^{-1}) is the rate constant for pseudo-second-order, q_e and q_t are the amounts of dye adsorbed per gram of adsorbent (mg.g^{-1}) at equilibrium and any time t. The intercept and slope form the plot t versus t/q_t were used to calculate the value of k_2 and $q_{e,cal}$.

The pseudo-first-order and pseudo-second-order kinetics plots for both TFC and BFC as

Table 3. Comparisons of different adsorbents in their effectiveness of methylene blue adsorption capacities.

Adsorbents	Surface area (m^2.g^{-1})	Methylene Blue Removal Capacity (mg.g^{-1})	References
Torrefied rice husk	28	6.82	[37]
TiO_2-sulfonated carbon-derived from *Eichhornia crassipes*	233	18.8	[26]
Alkaline treated Kaolinite	-	20.5	[38]
Carbon-derived *Tenggiri* fish bone	90.8	24.8	Present study
Carbon-derived *Belida* fish bone	131.7	20.8	Present study
Carbon nanotubes	160	26.1 – 41.6	[39]
Activated Bledug Kuwu	70	40.0	[40]
Calcined-fish bone waste	159	56.5	[27]
Graphene Oxide/Alginate	7.61	225.5	[41]
Chitosan/Graphene Oxide	-	107.1 – 179.6	[42]
Bamboo-based activated carbon	1896	454.2	[43]
Poly(acrylic acid) hydrogel	-	2100	[44]

adsorbent of methylene blue dye were checked with equations (4) and (5), respectively. The rate constant (k), equilibrium sorption calculated ($q_{e,cal}$) were determined by slope and intercept of the plots. Completely, the value of rate constant (k), equilibrium sorption calculated ($q_{e,cal}$), equilibrium sorption experiment ($q_{e,exp}$) and the correlation coefficients (R^2) were listed in Table 4. The value of the correlation coefficient (R^2) for pseudo-first-order of TFC and BFC as 0.814 and 0.540 were lower compared to the value for pseudo-second-order of both adsorbents by 1.000, where the pseudo-second-order indicates more accurate. This phenomenon is in line with the report by Ho and McKay [50] that concluded the first order equation of Lagergren is not well-suited for the whole range of contact time and is generally applicable over the initial stage of the adsorption process in many cases. The result of this research showed that the adsorption of methylene blue onto BFC adsorbents did not follow the pseudo-first-order kinetic.

Both adsorbent follow pseudo-second-order models also can be proven by the difference in $q_{e,cal}$ with $q_{e,exp}$ for both adsorbents in pseudo-second-order were lower compared with pseudo-first-order. Therefore, the adsorption of methylene blue dye onto both adsorbents were concluded to follow the pseudo-second-order adsorption mechanism model.

3.4 Adsorption Isotherms

The Langmuir and the Freundlich isotherm were used to identify the adsorption isotherm in adsorption process onto TFC and BFC adsorbent. The Langmuir isotherm is correlated with monolayer sorption onto a surface that equation is given by [51–53]:

$$\frac{C_e}{q_e} = \frac{1}{Q_{max}} C_e + \frac{1}{Q_{max}.b} \quad (6)$$

where, C_e and q_e are the residual dye concentration ($mg.L^{-1}$) and the number of the dye adsorbed on the sorbent at equilibrium ($mg.g^{-1}$). Meanwhile, Q_{max} and b are Langmuir constant which correlated with maximum adsorption capacity and bonding energy of adsorption, respectively. The slope and intercept of the linier plot of C_e/q_e versus C_e was used to determine Q_{max} and b.

The Freundlich isotherm model assumes heterogeneous site energies of sorption. The Freundlich equation is followed as [30,52]:

$$\ln q_e = \ln K_F + \left(\frac{1}{n}\right) \ln C_e \quad (7)$$

where, K_F and n are the Freundlich constant which indicate adsorption capacity and adsorption intensity, respectively. K_F ($mg.g^{-1}$) and n $(L.mg^{-1})^{1/n}$ were calculate from the intercept and slope of the plot of ln q_e versus ln C_e.

At equilibrium, the methylene blue removal capacity increased from 9.3 to 20.8 $mg.g^{-1}$ for BFC and 9.9 to 24.4 $mg.g^{-1}$ when the initial concentration of both dyes increased from 100 to 400 $mg.L^{-1}$. The increasing of the amount of dye removal at equilibrium condition was caused by an increasing the initial concentration that can increase the driving force to reduce all mass transfer resistances of the methylene blue molecules between the aqueous and solid phase of the adsorbent [54].

The Langmuir and the Freundlich adsorption isotherms were used to describe the interaction between the dye and adsorbent that follow equations (6) and (7), respectively. For the removal of methylene blue by TFC and BFC adsorbents, 25 mL of various dyes concentrations (between 100 and 400 $mg.L^{-1}$) were mixed with 0.250 mg sorbent, then stirred at 300 rpm for 240 min at room temperature. From the Langmuir equation can be calculated the value of the constants of Q_{max}, b and R^2 as 24.8 $mg.g^{-1}$, 0.257 and 0.9986 for TFC and 20.8 $mg.g^{-1}$, 0.0889 and 0.9999 for BFC, respectively. Base on the value of maximum adsorption capacity (Q_{max}), bonding energy (b) can be used to conclude that adsorption of methylene blue onto TFC was easier than BFC adsorbent.

The favorable adsorption onto adsorbent was investigated base on the constant K_F, n and R^2 were determined from the Freundlich isotherm that was obtained 10.752, 5.831 and

Table 4. First order and pseudo second order kinetics for methylene blue dyes adsorption on TFC and BFC adsorbent.

Dye removal	Temp. (°C)	First Order			Pseudo Second Order			$q_{e,exp}$ ($mg.g^{-1}$)
		$q_{e,cal}$ ($mg.g^{-1}$)	k_1 ($g.mg^{-1}.h^{-1}$)	R^2	$q_{e,cal}$ ($mg.g^{-1}$)	k_2 ($g.mg^{-1}.h^{-1}$)	R^2	
TFC	30	0.4573	0.0347	0.8141	9.9800	0.2431	1.000	9.9652
BFC	30	0.6086	0.0184	0.5404	9.3197	0.1247	1.000	9.2855

0.9813 for TFC and 6.086, 4.087 and 0.9765 for BFC, respectively. Base on K_F value can be concluded that the methylene blue adsorption process was the heterogeneous adsorption process on the surface of onto TFC and BFC adsorbent which was done through a multi-layer adsorption mechanism. The n values of methylene blue adsorption process are more than 1, which indicates favorable adsorption of both dyes onto TFC and BFC adsorbents. The complete data of Langmuir and the Freundlich isotherm were listed in Table 5.

3.5 Effect of Temperature

The thermodynamic parameters free energy (ΔG), enthalpy (ΔH) and entropy (ΔS) were determined by the experiments that were created at different temperatures. The value changes of ΔH and ΔS of adsorption were estimated from Van't Hoff equation [6,55]:

$$\ln K_C = -\frac{\Delta H}{R}\frac{1}{T} + \frac{\Delta S}{R} \quad (8)$$

with $K_C = C_1/C_2$, is the equilibrium constant and T, R, C_1 and C_2 are temperature (K), the gas constant (8.314 J.K^{-1}.mol^{-1}), the quantity of methylene blue dye adsorbed per unit mass of adsorbent and the concentration of methylene blue dye in aqueous phase, respectively. The linier plot of ln K_C versus 1/T was used to determine of ΔS and ΔH which calculated from the slope and intercept. The positive value of ΔS indicates that the increase in randomness of ongoing process. The negative value of ΔH indicates that the adsorption process is exothermic in nature and otherwise, the positive value of ΔH indicates that the adsorption process is endothermic in nature. Furthermore, the value of ΔG was calculated by using the equation $\Delta G^0 = \Delta H - T\Delta S$. The negative value of ΔG at each temperature shows the feasibility and spontaneity of adsorption process.

The Arrhenius equation was used to determine activation energy (E_a) for adsorption process onto TFC and BFC adsorbent. The equation is given as [30,55]:

$$\ln k = \ln A - \frac{E_a}{RT} \quad (9)$$

k, E_a (kJ.mol^{-1}), T (K), R (J.mol^{-1}.K^{-1}) and A are the rate constant, Arrhenius activation energy, temperature of the adsorption medium, the ideal gas constant (8.314 J.mol^{-1}.K^{-1}), and the Arrhenius factor, respectively. The slope of plotting ln k versus 1/T was used to calculate the Arrhenius activation energy. The removal of MB dye at varying temperatures increased from 94.2 to 99.6% (at room temperature), 93.3 to 99.3% (40 °C) and 92.8 to 98.5% (50 °C). It can be clearly seen that by increasing the temperature, the removal percentage of methylene blue dye decreased slowly.

The thermodynamic parameter value of ΔG, ΔH and ΔS are calculated based on the slope and intercept of Van't Hoff's plots follow equation (8). The value of ΔG, ΔH, and ΔS were listed in Table 6. The feasibility and spontaneity of ongoing MB adsorption onto TFC adsorbent was proven by negative value of free energy (ΔG). The negative value of enthalpy (ΔH) indicates that the adsorption process of MB onto TFC adsorbent is exothermic in nature. The activation energy (E_a) for adsorption process onto TFC adsorbent was calculated by the Arrhenius equation (9). The activation energy value for adsorption process onto TFC adsorbent was 7.157 kJ.mol^{-1}.

4. Conclusions

In this study, modified fishbone (Tenggiri and Belida) to be carbon (TFC and BFC) adsorbent has been carried out via a simple thermal activation method. The thermal activation was conducted at a carbonation temperature 500 °C

Table 5. Langmuir and Freundlich Isotherm models for methylene blue dyes adsorption on TFC and BFC adsorbent.

Adsorbent	Langmuir Isotherm			Freundlich Isotherm		
	Q_{max}	b	R^2	K_F	n	R^2
TFC	24.752	0.2568	0.998	10.752	5.831	0.9813
BFC	20.790	0.0889	0.999	6.086	4.087	0.9765

Table 6. Thermodynamic parameters data.

Adsorbent	ΔH (kJ/mol)	ΔS (kJ/mol.K)	ΔG (kJ/mol)			E_a (kJ/mol)
			30 °C	40 °C	50 °C	
TFC	−59.5	−0.149	−14.3	−12.8	−11.3	7.157

for 2 h. The surface area and pore size of TFC and BFC were 90.8 $m^2.g^{-1}$, 5.2 nm and 131.7 $m^2.g^{-1}$, 4.3 nm, respectively. Both carbon functions as an adsorbent for the methylene blue, one of the major pollutants from dye industries. The adsorption process was carried out by batch system at room temperature with the adsorbent (0.25 g) and methylene blue dye solution (25 mL, 100 $mg.L^{-1}$). The adsorption of methylene blue onto TFC and BFC follows the Langmuir adsorption isotherm with the maximum adsorption capacity 24.8 $mg.g^{-1}$ and 20.8 $mg.g^{-1}$. The kinetic data for methylene blue fitted with a pseudo-second-order model with rate constant calculated 0.243 $g.mg^{-1}.h^{-1}$ (TFC) and 0.125 $g.mg^{-1}.h^{-1}$ (BFC) at 30 °C. The enthalpy (ΔH) of methylene blue adsorption was obtained as −59.5 $kJ.mol^{-1}$ and the adsorption process was exothermic. The adsorption of methylene blue onto the TFC is spontaneous as predicted from the Gibbs free energy (ΔG) as −14.3 $kJ.mol^{-1}$ at 30 °C. In conclusion, carbon synthesized from fish bone can be a potential low-cost adsorbent for removing methylene blue.

Acknowledgements

The authors gratefully acknowledge research grant from *Fakultas Keguruan dan Ilmu Pendidikan*, Universitas Mulawarman, Year 2022 by contract number: 800/UN17.5/PG/2022, and research grant from *Kementerian Pendidikan, Kebudayaan, Riset dan Teknologi,* Republic of Indonesia by contract number: 297/UN17.L1/HK/2022.

References

[1] Karaoglu, M.H., Dogan, M., Alkan, M. (2010). Removal of Reactive Blue 221 by Kaolinite from Aqueous Solution. *Industrial & Engineering Chemistry Research,* 49(4), 1534–1540. DOI: 10.1021/ie9017258.

[2] Kumar, P.S., Ramalingam, S., Sathishkumar, K. (2011). Removal of methylene blue dye from aqueous solution by activated carbon prepared from cashew nut shell as a new low-cost adsorbent. *Korean Journal of Chemical Engineering*, 28, 149–155. DOI: 10.1007/s11814-010-0342-0.

[3] Yi, J.-Z., Zhang, L.-M. (2008). Removal of methylene blue dye from aqueous solution by adsorption onto sodium humate/polycrylamide/cly hybrid hydrogels. *Bioresource Technology,* 99, 2182–2186. DOI: 10.1016/j.biortech.2007.05.028.

[4] Danish, M., Ahmad, T. (2018). A review on utilization of wood biomass as a sustainable precursor for activated carbon production and application. *Renewable and Sustainable Energy Reviews,* 87, 1–21. DOI: 10.1016/j.rser.2018.02.003.

[5] Zhao, Y., Xue, Z., Wang, X., Li, W., Aiqin, W. (2012). Adsorption of Congo Red onto Lognocellulose/Montmorillonite Nanocomposite. *Journal of Wuhan University of Technology-Mater. Sci. Ed.,* 27(5), 931–938. DOI: 10.1007/s11595-012-0576-2.

[6] Gao, J.-j., Qin, Y.-b., Zhou, T., Cao, D.-d., Xu, P., Hochstetter, D., Yue-fei, W., (2013). Adsorption of methylene blue onto activated carbon produced from tea (Camellia sinensis L.) seed shells: kinetics, equilibrium, and thermodynamics studies. *Journal of Zhejiang University SCIENCE B,* 14(7), 650–658. DOI: 10.1631/jzus.B12a0225.

[7] Al-Qodah, Z. (2000). Adsorption of dyes using shale oil ash. *Water Research,* 34(17), 4295-4303. DOI: 10.1016/S0043-1354(00)00196-2.

[8] Nigam, P., Armour, G., Banat, I.M., Singh, D., Marchant, R. (2000). Physical removal of textile dyes from effluents and solid-sate fermentation of dye-adsorbed agriculturalresidues. *Bioresource Technology,* 72, 219-226. DOI: 10.1016/S0960-8524(99)00123-6.

[9] Gupta, G.S., Prasad, G., Panday, K.K., Singh, V.N. (1988). Removal of chrome dye from aqueous solution by fly ash. *Water, Air, and Soil Pollution,* 37, 13–24. DOI: 10.1007/BF00226476.

[10] Sun, Q., Yang, L. (2003). The adsorption of basic dyes from aqueous solution on modified peat-resin particle. *Water Research,* 37, 1535-1544. DOI: 10.1016/S0043-1354(02)00520-1.

[11] Pavan, F.A., Mazzocato, A.C., Gushikem, Y. (2008). Removal of methylene blue dye from aqueous solution by adsorption using yellow passion fruit peel as adsorbent. *Bioresource Technology,* 99, 3162-3165. DOI: 10.1016/j.biortech.2007.05.067.

[12] Giri, A.K., Patel, R., Mandal, S. (2012). Removal of Cr(VI) from aqueous solution by Eichhornia crassipes root biomass-derived activated carbon. *Chemical Engineering Journal,* 185-186, 71-81. DOI: 10.1016/j.cej.2012.01.025.

[13] Acemioglu, B., Almay, M.H. (2001). Equilibrium Studies on Adsorption of Cu(II) from Aqueous Solution onto Cellulose. *Journal of Colloid and Interface Science,* 243, 81-84. DOI: 10.1006/jcis.2001.7873.

[14] Hasan, V., Mukti, A.T., Putranto, T.W. (2019). Range expansion of the invasive nile tilapia oreochromisniloticus (perciformes: cichlidae) in Java Sea and first record for Kangean Island, Madura, East Java, Indonesia. *Ecology, Environment and Conservation,* 25, 187-189.

[15] Kusumawardani, R., Nurhadi, M., Wirawan, T., Prasetyo, A., Agusti, N.N., Lai, S.Y., Hadi, N., (2022). Kinetic Study of Styrene Oxidation over Titania Catalyst Supported on Sulfonated Fish Bone-derived Carbon. *Bulletin of Chemical Reaction Engineering & Catalysis,* 17(1), 194-204. DOI: 10.9767/bcrec.17.1.13133.194-204.

[16] Szpak, P. (2011). Fish bone chemistry and ultrastructure: implications for taphonomy and stable isotope analysis. *Journal of Archaeological Science,* 38(12), 3358-3372. DOI: 10.1016/j.jas.2011.07.022.

[17] Cahyanto, A., Kosasih, E., Aripin, D., Hasratiningsih, Z. (2017). Fabrication of hydroxyapatite from fish bones waste using reflux method. *IOP Conference Series: Materials Science and Engineering,* 172, 012006. DOI: 10.1088/1757-899X/172/1/012006.

[18] Lairah, V.P.J., Wuntu, A.D., Aritonang, H.F. (2021). Synthesis of Ag_3PO_4/HAp from Red Snapper Bone (Lutjanus spp.) For Photodegradation of Methylene Blue. *IOP Conference Series: Materials Science and Engineering,* 1115, 012082. DOI: 10.1088/1757-899X/1115/1/012082.

[19] Andriyan, M.W., Alfatinnisa, Z., Patmala, D., Amalia, F.M., Shinta, A., Subagio, A. (2022). Effectiveness Study of Using HAp Milkfish Bone to Synthesize Ag_3PO_4 with Ion-Exchange Method for Methylene Blue Degradation. *Key Engineering Materials*, 920, 14-21. DOI: 10.4028/p-ksfb64.

[20] Tan, Y.H., Abdullah, M.O., Kansedo, J., Mubarak, N.M., Chan, Y.S., Nolasco-Hipolito, C. (2019). Biodiesel production from used cooking oil using green solid catalyst derived from calcined fusion waste chicken and fish bones. *Renewable Energy,* 139, 696-706. DOI: 10.1016/j.renene.2019.02.110.

[21] Chinglenthoiba, C., Das, A., Vandana, S. (2020). Enhanced biodiesel production from waste cooking palm oil, with NaOH-loaded Calcined fish bones as the catalyst. *Environmental Science and Pollution Research,* 27, 15925-15930. DOI: 10.1007/s11356-020-08249-7.

[22] Wang, W., Liu, Y.-y., Chen, X.-f., Song, S.-x. (2018). Facile Synthesis of NaOH-modified Fishbone Charcoal (FBC) with Remarkable Adsorption towards Methylene Blue. *Procedia Engineering,* 211, 495-505. DOI: 10.1016/j.proeng.2017.12.041

[23] Wang, Y., Peng, Q., Akhtar, N., Chen, X., Huang, Y. (2020). Microporous carbon material from fish waste for removal of methylene blue from wastewater. *Water Science and Technology*, 81(6), 1180-1190. DOI: 10.2166/wst.2020.211.

[24] Parvin, S., Hussain, M.M., Akter, F., Biswas, B. K. (2021). Removal of Congo Red by Silver Carp (Hypophthalmichthys molitrix) Fish Bone Powder: Kinetics, Equilibrium, and Thermodynamic Study. *Journal of Chemistry,* 2021, 1-11. DOI: 10.1155/2021/9535644

[25] Nurhadi, M., Kusumawardani, R., Wirawan, T., Sumari, S., Lai, S.Y., Nur, H. (2021). Catalytic Performance of TiO_2–Carbon Mesoporous_Derived from Fish Bones in Styrene Oxidation with Aqueous Hydrogen Peroxide as an Oxidant. *Bulletin of Chemical Reaction Engineering & Catalysis,* 16(1), 88-96. DOI: 10.9767/bcrec.16.1.9729.88-96.

[26] Widiyowati, I.I., Nurhadi, M., Hatami, M., Yuan, L.S. (2020). Effective TiO_2-Sulfonated Carbon-derived from Eichhornia crassipes in The Removal of Methylene Blue and Congo Red Dyes from Aqueous Solution. *Bulletin of Chemical Reaction Engineering & Catalysis,* 15(2), 476-489. DOI: 10.9767/bcrec.15.2.6997.476-489.

[27] Kusumawardani, R., Nurhadi, M., Wirhanuddin, Gunawan, R., Nur, H. (2019). Carbon-containing Hydroxyapatite Obtained from Fish Bone as Low-cost Mesoporous Material for Methylene Blue Adsorption. *Bulletin of Chemical Reaction Engineering & Catalysis,* 14(3), 660-671. DOI: 10.9767/bcrec.14.3.5365.660-671.

[28] Wanyonyi, W.C., Onyari, J.M., Shiundu, P.M. (2014). Adsorption of Congo Red Dye from Aqueous Solution Using Roots of Eichhornia Crassipes: Kinetic and Equilibrium Studies *Energy Procedia,* 50, 862-869. DOI: 10.1016/j.egypro.2014.06.105.

[29] Nurhadi, M., Widiyowati, I.I., Wirhanuddin, Chandren, S. (2019). Kinetic of Adsorption Process of Sulfonated Carbon-derived from Eichhornia crassipes in the Adsorption of Methylene Blue Dye from Aqueous Solution. *Bulletin of Chemical Reaction Engineering & Catalysis,* 14(1), 17-27. DOI: 10.9767/bcrec.14.1.2548.17-27.

[30] Pathania, D., Sharma, A., Siddiqi, Z.M. (2016). Removal of congo red dye from aqueous system using Phoenix dactylifera seeds. *Journal of Molecular Liquids,* 219, 359-367. DOI: 10.1016/j.molliq.2016.03.020.

[31] Chakraborty, R., Roy Chowdhury, D. (2013). Fish bone derived natural hydroxyapatite-supported copper acid catalyst: Taguchi optimization of semibatch oleic acid esterification. *Chemical Engineering Journal*, 215–216, 491–499. DOI: 10.1016/j.cej.2012.11.064.

[32] Patel, S., Han, J., Qiu, W., Gao, W. (2015). Synthesis and characterisation of mesoporous bone char obtained by pyrolysis of animal bones, for environmental application. *Journal of Environmental Chemical Engineering*, 3, 2368-2377. DOI: 10.1016/j.jece.2015.07.031.

[33] Yin, T., Park, J.W., Xiong, S. (2015). Physico-chemical properties of nano fish bone prepared by wet media milling. *LWT - Food Science and Technology*, 64(1), 367-373. DOI: 10.1016/j.lwt.2015.06.007.

[34] Zayed, E.M., Sokker, H.H., Albishri, H.M., Farag, A.M. (2013). Potential use of novel modified fishbone for anchoring hazardous metal ions from their solutions. *Ecological Engineering,* 61, 390–393. DOI: 10.1016/j.ecoleng.2013.09.010.

[35] Boutinguiza, M., Poua, J., Comesaña, R., Lusquiños, F., Carlos, A.d., Leóna, B. (2012). Biological hydroxyapatite obtained from fish bones. *Materials Science and Engineering: C,* 32(3), 478-486. DOI: 10.1016/j.msec.2011.11.021.

[36] Jaber, H.L., Hammood, A.S., Parvin, N. (2017). Synthesis and characterization of hydroxyapatite powder from natural Camelus bone. *Journal of the Australian Ceramic Society,* 54(1), 1-10. DOI: 10.1007/s41779-017-0120-0.

[37] Hummadi, K.K., Luo, S., He, S. (2022). Adsorption of methylene blue dye from the aqueous solution via bio-adsorption in the inverse fluidized-bed adsorption column using the torrefied rice husk *Chemosphere,* 287(1), 131907. DOI: 10.1016/j.chemosphere.2021.131907.

[38] Hofmann, U., Kottenhahn, H., Morcos, S. (1966). Morcos, Adsorption of Methylene Blue on Clays. *Angewandte Chemie International Edition,* 5(2), 247-248. DOI: 10.1002/anie.196602473.

[39] Yao, Y., Xu, F., Chen, M., Xu, Z., Zhu, Z. (2010). Adsorption behavior of methylene blue on carbon nanotubes. *Bioresource Technology,* 101(9), 3040-3046. DOI: 10.1016/j.biortech.2009.12.042.

[40] Lestari, S., Muflihah, M., Kusumawardani, R., Nurhadi, M., Mangesa, Y., Ridho, F.I., Adawiyah, R., Ambarwati, P., Rahma, S., Sin Yuan Lai, S.Y., Nur, H. (2022). Activated Bledug Kuwu's Clay as Adsorbent Potential for Synthetic Dye Adsorption: Kinetic and Thermodynamic Studies. *Bulletin of Chemical Reaction Engineering and Catalysis,* 17(1), 22-31. DOI: 10.9767/bcrec.17.1.12473.22-31.

[41] Fadillah, G., Saleh, T.A., Wahyuningsih, S., Putri, E.N.K., Febrianastuti, S. (2019). Electrochemical removal of methylene blue using alginate-modified graphene adsorbents. *Chemical Engineering Journal,* 378, 122140. DOI: 10.1016/j.cej.2019.122140.

[42] Fan, L., Luo, C., Sun, M., Li, X., Lu, F., Qiu, H. (2012). Preparation of novel magnetic chitosan/graphene oxide composite as effective adsorbents toward methylene blue. *Bioresource Technology,* 114, 703-706. DOI: 10.1016/j.biortech.2012.02.067.

[43] Hameed, B.H., Din, A.T.M., Ahmad, A.L. (2007). Adsorption of methylene blue onto bamboo-based activated carbon: Kinetics and equilibrium studies. *Journal of Hazardous Materials,* 141(3), 819-825. DOI: 10.1016/j.jhazmat.2006.07.049.

[44] Hu, X.-S., Lianga, R., Sun, G. (2018). Super-adsorbent hydrogel for removal of methylene blue dye from aqueous solution. *Journal of Materials Chemistry A,* 6, 17612-17624. DOI: 10.1039/C8TA04722G.

[45] Aksu, Z. (2005). Application of biosorption for the removal of organic pollutants: a review. *Process Biochemistry,* 40, 997-1026. DOI: 10.1016/j.procbio.2004.04.008.

[46] Lim, H.K., Teng, T.T., Ibrahim, M.H., Ahmad, A., Chee, H.T. (2012). Adsorption and Removal of Zinc (II) from Aqueous Solution Using Powdered Fish Bones. *APCBEE Procedia,* 1, 96-102. DOI: 10.1016/j.apcbee.2012.03.017.

[47] Mohanty, K., Jha, M., Meikap, B.C., Biswas, M.N. (2006). Biosorption of Cr(VI) from aqueous solutions by Eichhornia crassipes. *Chemical Engineering Journal,* 117, 71–77. DOI: 10.1016/j.cej.2005.11.018.

[48] Mahmoodi, N.M., Khorramfar, S., Najafi, F. (2011). Amine-functionalized silica nanoparticle: Preparation, characterization and anionic dye removal ability. *Desalination,* 279, 79-87. DOI: 10.1016/j.desal.2011.05.059.

[49] Ho, Y.S., McKay, G. (1999). Pseudo-second order model for sorption processes. *Process Biochemistry,* 34, 451-465. DOI: 10.1016/S0032-9592(98)00112-5.

[50] Ho, Y.S., McKay, G. (1998). Sorption of dye from aqueous solution by peat. *Chemical Engineering Journal,* 70, 115-124. DOI: 10.1016/S0923-0467(98)00076-1.

[51] Khaniabadi, Y.O., Basiri, H., Nourmoradi, H., Mohammadi, M.J., Yari, A.R., Sadeghi, S., Amrane, A. (2017). Adsorption of Congo Red Dye From Aqueous Solutions by Montmorillonite as a Low-cost Adsorbent. *International Journal of Chemical Reactor Engineering,* 16(1), 1-11. DOI: 10.1515/ijcre-2016-0203.

[52] Sharma, P.K., Ayub, S., Tripathi, C.N. (2016). Isotherm describing physical adsorption of Cr(VI) from aqueous solution using various agricultural wastes as adsorbent. *Cogent Engineering*, 3, 1-20. DOI: 10.1080/23311916.2016.1186857.

[53] Baccar, R., Blangquez, P., Bouzid, J., Feki, M., Sarra, M. (2010). Equilibrium, thermodynamic and kinetic studies on adsorption of commercial dye by activated carbon derived from olive-waste cakes. *Chemical Engineering Journal*, 165(2), 457-464. DOI: 10.1016/j.cej.2010.09.033.

[54] Wanyonyi, W.C., Onyari, J.M., Shiundu, P.M. (2013). Adsorption of Methylene Blue Dye from Aqueous Solution Using Eichhornia crassipes. *Bulletin of Environmental Contamination and Toxicology*, 91, 362-366. DOI: 10.1007/s00128-013-1053-0.

[55] Yang, L., Zhang, Y., Liu, X., Jiang, X., Zhang, Z., Zhang, T., Zhang, L. (2014). The Investigation of Synergistic and competitive interaction between dye Congo red and Methyl blue on magnetic $MnFe_2O_4$. *Chemical Engineering Journal*, 246, 88-96. DOI: 10.1016/j.cej.2014.02.044